

Wind Tunnel Design and Operation



By: Nathan Tatman

Mentor: Dr. Rhett Herman

Wind Tunnel Design and Operation

This paper will focus primarily on the design and operation of low speed wind tunnels. The components involved in the construction of a typical wind tunnel will be presented and accompanied by brief commentary on the underlying physical processes most influential in determining optimal construction of each component. A summary overview of fluid dynamic principles concerning incompressible flow in tubes will include discussion on laminar and turbulent flow, fluid viscosity, Reynolds number criteria, and boundary layer formation. I will also be presenting data obtained from experimental research in the form of velocity profiles for the wind tunnel I constructed.

Development of the Wind Tunnel

When the first real scientific investigations into the fledgling field of aeronautics, scientists hoping to achieve heavier than air flight soon realized that they would need to understand airflow dynamics about an airfoil in order to design a practical wing. In order to do this, they would need to reliably measure forces acting on a body passing quickly through the air. Until the early 1700s, natural wind sources such as high ridges and the mouths of caves were used for early testing, but these proved to be inadequate, and so a mechanical means of creating airflow was invented, the so-called whirling arm apparatus. An English mathematician named Benjamin Robins is credited as being the first to use a whirling arm for aeronautical study. The apparatus was driven by falling weights attached via a system of ropes and pulleys to a long arm, which rotated horizontally about a spindle. Test bodies were attached to the tip of the arm and could be positioned so as to obtain varying angles of attack. Robins' first whirling arm was four feet in length, and the tip reached speeds of only a few feet per second, but longer arms could obtain speeds of up to 20 feet per second.

Over the next hundred years whirling arms grew larger and eventually steam engines replaced the falling weights, enabling researchers to obtain tip speeds in excess of 100 mph. Despite this impressive performance, whirling arms were not without their flaws. Some of the larger arm were constructed out of doors and so were still susceptible to the effects of natural winds. But regardless of location, all whirling arms suffered from a common shortcoming – the revolving arm disturbed nearby air, causing it to begin rotating around the apparatus. In addition to this loss of quiescence, results also suffered because the test body experienced appreciable amounts of turbulence caused by repeatedly passing through its own wake.

In 1871, dissatisfaction with the whirling arms led Frank H. Wenham to design and built a twelve foot long blower tunnel with a steam powered fan. The success of Wenham's wind tunnel experiments inspired others interested powered flight to construct their own tunnels. Sir Hiram Maxim used money made from the success of his machine gun to construct a wind tunnel with a three-foot diameter, twice the size of Wehham's, which was powered by a pair of axial fan and capable of airspeeds on the order of 50

mph. Using data from this tunnel Maxim successfully developed and twin engine test plane. The wing design proved so effective that during one test on July 31, 1894 the plane, carrying three passengers, accidentally broke free from its restraining rails and achieved the first powered (albeit uncontrolled) flight, a full decade before the Wright brothers.

The Wright brothers also made extensive use of a wind tunnel during the development of their third flyer after their first two failed to meet their expectations. This was due in large part to the fact that they were trying to apply lift tables compiled by Otto Lilienthal to wing designs very different from those for which they were intended. The Wright brothers interpreted the deviation from their anticipated results as an error in Lilienthal's tables, despite the fact that the German engineer had already design several successful hang gliders with only a whirling arm to collect data, and so built their own six foot wind tunnel. Though their tunnel and measuring devices were rather crude, the Wrights were able to produce data accurate to one tenth of a degree (the Wrights used a balance and scale systems to make measurement). The brother's tabular compilation of their data, especially lift to drag ratios of over 200 wing designs was a substantial step forward in aeronautical science. Thus, despite the relatively crude design of these early wind tunnels, they had proven to be invaluable tools for gaining a deeper understanding of aerodynamic principles.

Fluid Dynamics

Ideal/Real Fluid

An ideal fluid is a fluid that that experiences no viscous forces. This property of inviscid fluids allow them to flow along walls without an velocity decay due to skin friction, and also eliminates drag on adjacent lamina due to velocity gradients. This in turn means that ideal fluids do not form turbulent vortices as these flow past obstructions. Ideal fluids can be thought of as body of tiny frictionless particles, capable of supporting pressures at normal incidence but unaffected by shearing stresses. Ideal fluids are strictly a theoretical conception, but are sometime useful in modeling real-world situations where viscous forces can be neglected to a reasonable approximation. Viscous fluids more commonly found in practical situation are called real fluids, and though their analysis is a great deal more complex due to the addition of viscous forces, they are use in a far broader range of applications.

Laminar/Turbulent Flow

Laminar flow is the movement of fluid in thin parallel layers who slide one over the other much like sheets of paper. Each layer experiences strong viscous forces from adjacent layers and these forces have a damping effect on disruptions in the flow so that flow downstream of an obstacle quickly returns to its undisturbed state.

Turbulent flow is the highly random and chaotic flow that occurs at high Reynolds numbers characterized by the formation of eddies and vortices of various sizes. Unlike laminar flow, in which fluid behavior is determined primarily by viscous forces, flow behavior in turbulent flow is determined by inertial forces. Calculating fluid behavior in turbulent flow is often very difficult, as the Navier-Stokes equations that must be used are very complex. These equations relate the pressure, density, temperature and velocity of a fluid through the use of rate of stress and strain tensors, and the result is a set of five coupled differential equations (an additional equation of state is also needed in order to find a solution). In all but the simplest of cases, these equations are extremely difficult to solve analytically, and most solutions must be found through approximations and the use of high speed computers.

Fluid Viscosity

Viscosity is often defined as a measure of how resistive a fluid is to flow or deformation. Viscosity can be likened somewhat to friction experienced by solid objects, but unlike the frictional forces between solids, viscous forces are independent of pressure. Viscosity is ultimately caused by cohesive intermolecular forces, and can be expressed mathematically as the ratio of shearing stress on a fluid to its velocity gradient. Viscosity can be observed in a number of common liquids. For example, maple syrup has a higher viscosity than water and so flows more slowly. Gases also experience viscous forces and these forces increase as the temperature of the gas increases. This is due to the fact that as temperature increases, so does the kinetic energy of the molecules and so there is an increase in rate of intermolecular collisions. To a good approximation, the viscosity of a gas goes as the square root of its temperature.

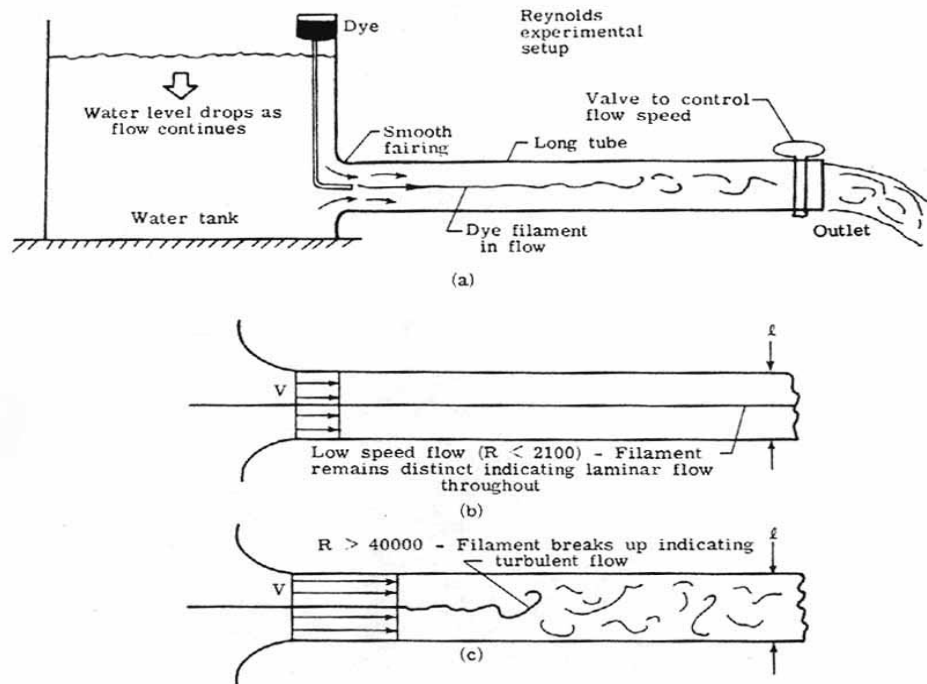
Skin Friction Drag

Skin friction drag is the component of the total drag, also called parasitic or profile drag, experienced by a body in a fluid flow due directly to frictional forces between the fluid and the surface of the body. Assuming no boundary layer separation occurs, skin friction is the sole source of friction.

Reynolds Number

Osborne Reynolds first introduced the dimensionless constant that bears his name in his 1883, in a paper he published in the Philosophical Transactions of the Royal Society. The paper, "An Experimental Investigation Of The Circumstances Which Determine Whether Motion Of Water Shall Be Direct Or Sinuous And Of The Law Of Resistance In Parallel Channels", detailed the findings of his experimental work.

Using an apparatus that allowed him to inject a small stream of dye into fluid flowing through a glass tube and using a manometer to determine flow velocities, Reynolds noticed that at lower flow velocities, the stream of dye remained intact but at higher velocities the coherent stream began to diffuse. He also noted that the diffused dye could be reformed into a stream if the velocity was decreased. Reynolds found that there was a critical velocity, which he termed the upper critical velocity, at which the turbulent flow developed and a lower critical velocity at which turbulent flow became laminar. Velocities located between these two points were classified as lying in the transition region.



Experimental setup similar to that used by Oscar Reynolds (1)

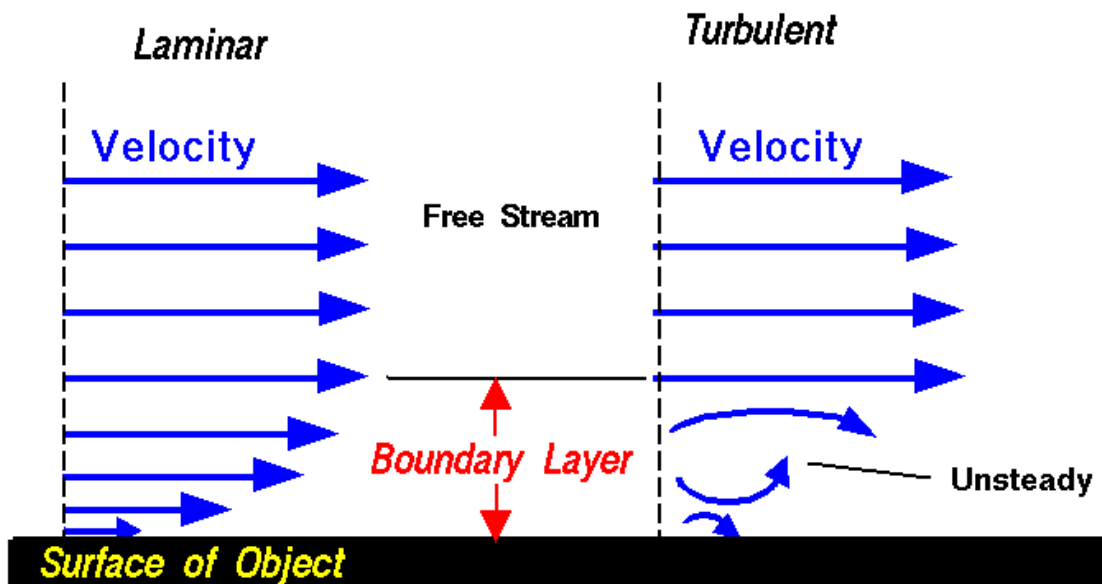
The Reynolds number itself is a dimensionless constant used to distinguish laminar from turbulent flow in a pipe or channel or sometime around an immersed object, with lower values corresponding to laminar flow and higher ones to turbulent flow. The Reynolds number is calculated using mean velocity, pipe diameter, density, and viscosity, and is valid for any fluid. The Reynolds number is also dependent upon the geometry of the pipe, as well as the roughness of the walls. Analysis of the Reynolds number using the dimensionless forms of the Navier Stokes equations reveals that the Reynolds number is really a ratio of inertial forces to viscous forces. As of yet, no successful analytic methods for determining Reynolds numbers have been developed due largely to the difficulty associated with predicting turbulent flow, and so Reynolds numbers for flow through pipes or around immersed objects must be determined experimentally.

Boundary Layers

Boundary layers are regions of fluid located immediately adjacent to an immersed object or wall in which flow velocities are governed by viscous forces. Drag forces and most of the heat exchange experienced by the object are due to fluid in this region. Boundary layers typically begin as a very thin region of laminar flow that thickens with increasing Reynolds numbers and then gradually transitions to a turbulent layer flowing over a viscous sublayer. Flow outside of the boundary layer is independent of Reynolds number criteria.



Boundary Layer



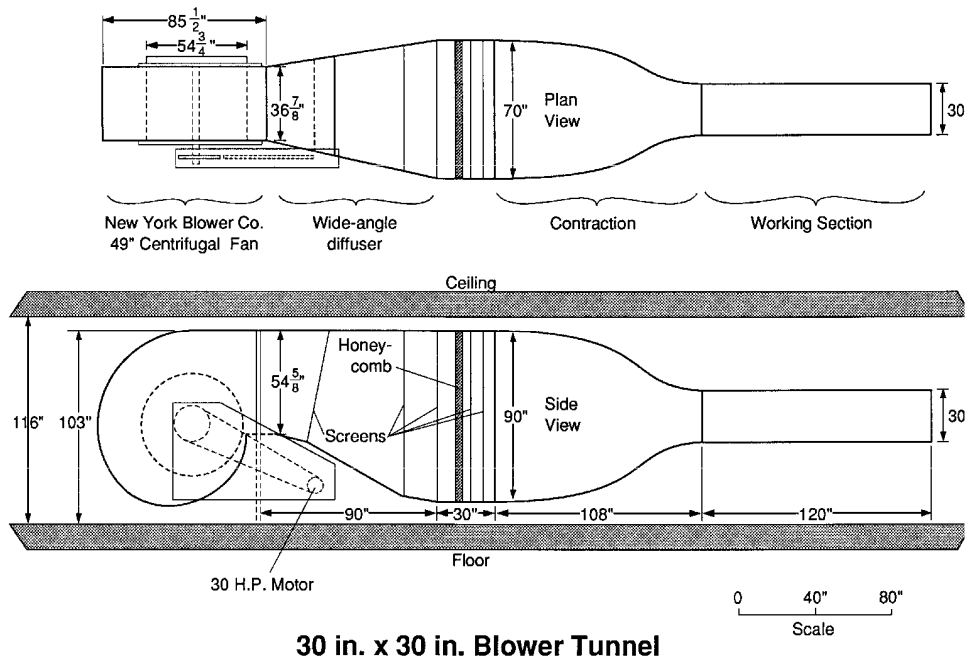
Velocity is zero at the surface (no - slip)

Velocity profile for boundary layers along a wall (2)

Wind Tunnel Basics

Basic Types (Open/Closed Circuit)

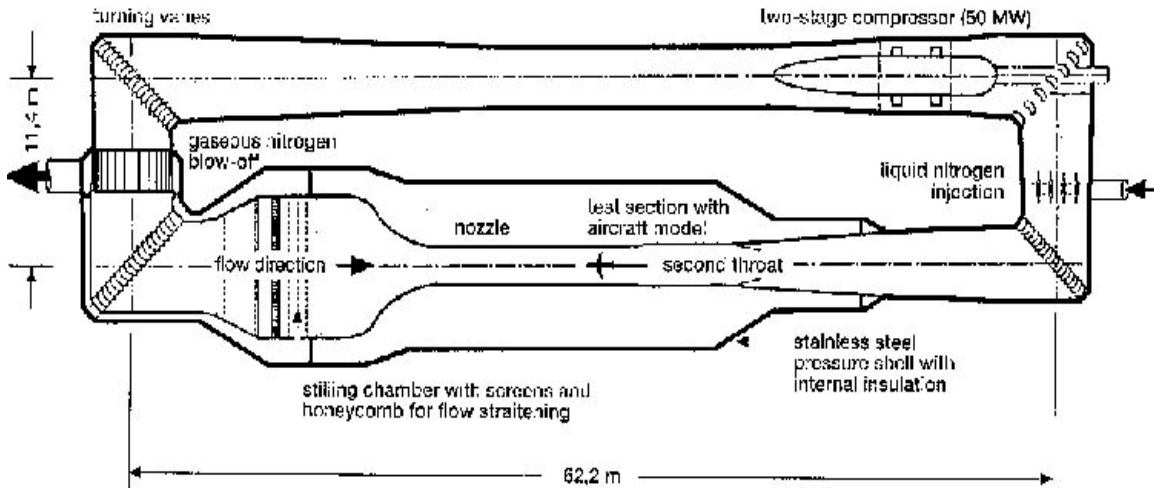
The open circuit wind tunnel is the simplest and most affordable to build. In these tunnels air is expelled directly into the laboratory and typically reingested after circulating through the lab, though some tunnels utilize instead a compressed gas source. In addition to their low costs, open circuit tunnels are also advantageous because they have are relatively immune to temperature fluctuations and large disturbances in return flow, provided that the volume of the laboratory is much greater than that of the tunnel.



30 in. x 30 in. Blower Tunnel

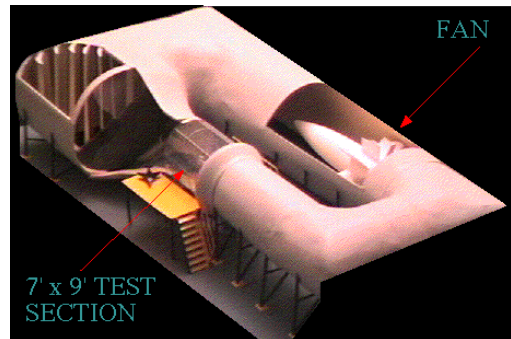
An open circuit blower tunnel. Notice that the exit diffuser has been omitted. (3)

There are two basic types of open circuit tunnels, “suckdown” and “blower,” and the two are most easily differentiated by the location of the fan. Blower tunnels are the most flexible because the fan is at the inlet of the tunnel, so the test section can be easily interchanged or modified with seriously disrupting flow. These tunnels are so forgiving that exit diffusers can often be completely omitted to allow easier access to test samples and instruments, though the omission often results in a noticeable power loss. Suckdown tunnels are typically more susceptible to low frequency unsteadiness in the return flow than blowers, though some claims have been made that intake swirl is less problematic in these tunnels because it does not pass through the fan before entering the test section.



Closed circuit wind tunnel. (4)

As the name implies, closed circuit tunnels (also called closed return) form an enclosed loop in which exhaust flow is directly returned to the tunnel inlet. These tunnels are usually larger and more difficult to build. They must be carefully designed in order to maximize uniformity in the return flow. These tunnels are powered by axial fan(s) upstream of the test section and sometimes include multistage compressors, which are often necessary to create trans- and supersonic air speeds.



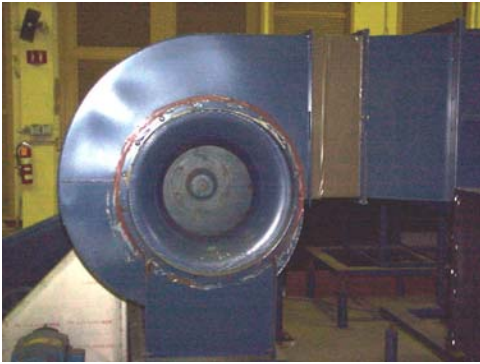
Cutaway of a closed circuit tunnel, the axial fan and corner vanes are visible. (5)

Fans

Axial fans are popular in open circuit tunnels, and are almost always found in closed circuit tunnels. In larger tunnels, pre-rotation vanes called stators are commonly positioned upstream of the fan, substantially decreasing swirl in the exit flow. Axial fans have a relatively limited effective operating range as the reduction in pressure increase through the fan as the blades approach stall speeds is far more abrupt than in centrifugal blowers. Care must also be given to choosing the proper blade size, shape and spacing in order to prevent shock wave production, stalling, and backflow.



A large axial flow fan. Notice the stators just upstream of the fan blades. (6)



A centrifugal blower. (7)

Centrifugal blowers, sometimes called squirrel cage blowers are most often in blower type open circuit tunnels, though they can be used in closed return tunnels if mounted in a corner. Centrifugal blowers have a much larger operating range than axial fans with acceptable levels of unsteadiness.

Settling Chamber

The settling chamber is located between the fan or wide angle diffuser and the contraction and contains the honeycombs and screens used to moderate longitudinal variations in the flow. Screens in the chamber should be spaced at 0.2 chamber diameters apart so that flow disturbed by the first screen can settle before it encounters the second.

Honeycombs

Honeycombs are located in the settling chamber and are used to reduce nonuniformities in the flow. For optimum benefit, honeycombs should be 6-8 cell diameters thick and cell size should be on the order of about 150 cells per settling chamber diameter.

Screens

Screens are typically located just downstream of the honeycomb and sometime at the inlet of the test section. Screens create a static pressure drop and serve to reduce boundary layer size and increase flow uniformity. A screen is characterized by its open-area ratio, which is defined in the equation below where d is the wire diameter and L is the length of the screen. At least one screen in the settling chamber (ideally the last) should have an open-area ratio of $\beta < 0.57$, as screens with lower ratios are known to produced nonuniformities in the flow. This is presumable due to the formation of small vortices created by the random coalescence of tiny jets emitted from the screen. The pressure drop across a screen depends upon the open-area ratio of the screen and the density, kinematic viscosity, and mean velocity of the fluid.

$$\beta = \left(1 - \frac{d}{L}\right)^2$$

Contraction Section

Contractions sections are located between the settling chamber and the test sections and serve to both increase mean velocities at the test section inlet and moderate inconsistencies in the uniformity of the flow. Large contraction ratios and short contraction lengths are generally more desirable as they reduce the power loss across the screens and the thickness of boundary layers. Small tunnels typically have contraction ratios between 6 and 9.

Test Section

The test section is the chamber in which measurements and observations are made and its shape and size are largely determined by the testing requirements. The test section should be long enough that flow disturbances resulting from a contraction or screens are sufficiently damped before reaching the test object. However, care should be taken not to make this section too long as this will lead to detrimental boundary layer growth which can separate when it enters the exit diffuser and create a power loss. This can be prevented by slightly enlarging the tunnel or by partially obstructing the exit end of the tunnel to create an overpressure which allows the use of small vents to control boundary layer growth.

Velocimeters/Observation Devices

A wide variety of velocity-measuring devices exist, and for the sake of brevity I will only touch on a few of the most popular. Pitot tubes are used to measure differences in pressure, usually with the aid of a manometer. In modern experimentation, it is common to utilize a device that combines a pitot tube with a static pressure measurement device so that both static pressure and stagnation pressure (total pressure) can be measured simultaneously. These devices are called pitot-static tubes, and can measure the difference in total and static pressure, from which velocities can be calculated using the relation between dynamic pressure and fluid velocity. (Total pressure is simply the sum of static and dynamic pressures.) When using pitot tubes, care must be taken with regard to proper orientation of the tube, as a difference of only a few degrees from parallel to the flow lines could alter readings.

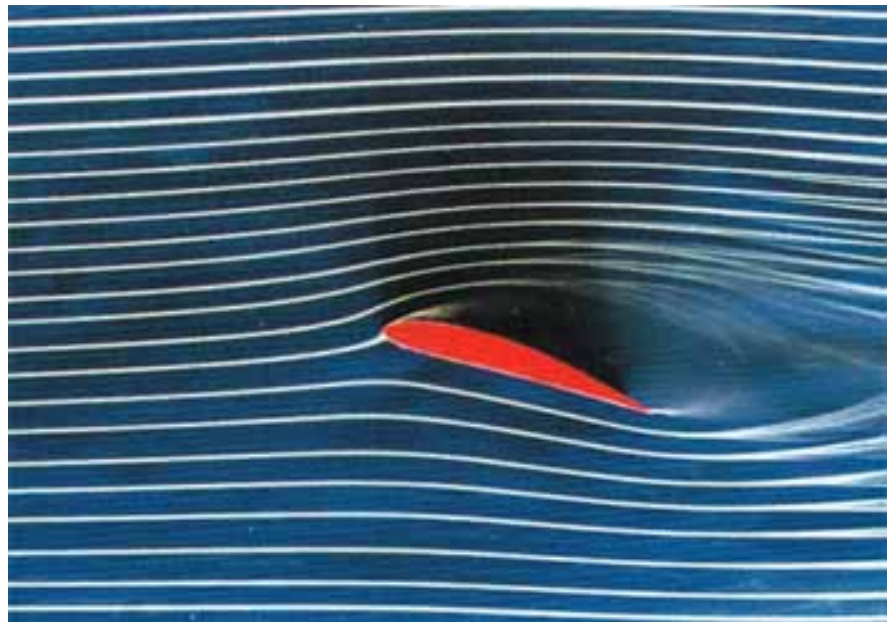
Anemometers are mechanical devices that measure air velocity through the use of rotating cups or vanes, and velocity can be determined by the speed of the rotation. Hot wire anemometers are electrical devices that measure heat loss due to fluid flowing over a conducting wire. These anemometers are currently among the most popular velocity measurement devices, and are also extremely sensitive. Using a properly controlled device in a constant temperature circuit, it is possible to take velocity measurements 500,000 times a second. Other devices used for velocity measurement include acoustic flowmeters and laser velocimeters. These devices detect velocities by either measuring the time taken for a pulse of known velocity to be reflected back to the detector,

or by measuring Doppler effects due to fluid flow. Though not always practical in application, these devices offer the huge advantage of detecting fluid velocity without causing disturbances in the flow.



Smoke passing over a scale model airframe illuminated by lasers. (8)

A number of visual aids are also used to qualitatively observe fluid flow in wind tunnels. The most popular are probably smoke and strings. Smoke can be introduced into the tunnel in a series of small streams or in a single stream emitted from the tip of a smooth probe. Small, lightweight strings are typically glued directly to the test body, but can also be attached to a moveable probe or to a wire grid positioned just downstream of the body.



Smoke streams passing over an airfoil. (9)

Diffuser

Diffusers are chambers that slowly expand along their length, allowing fluid pressure to increase and decreasing fluid velocity. Angles slightly larger than 5 degrees do increase pressure recovery, but can also lead to boundary layer separation and thus flow unsteadiness. Exit diffusers are located downstream of the test section and are used to recover pressure from kinetic motion of the fluid thereby reduced the power required to drive the tunnel.

Wide angle diffusers are located between the fan and the settling chamber and are necessary in order to facilitate the use of a beneficial contraction section, but the wide angle leads to boundary layer separation which must be controlled with the use of

screens. Diffusers are still not very well understood, and most of our working knowledge about them comes from experiment.

Corner Vanes

Corner vanes are thin curved blades usually made from sheet metal that are placed in the in corners of a tunnel, typically along the return circuit in a closed tunnel. Their purpose is to redirect flow while minimizing pressure loss and boundary layer separation.

My Wind Tunnel



Dimensions

Overall length – 10ft

Test Section Length – 32 in

Test Section Diameter – 10in

Settling Chamber Diameter – 32in

Contraction Ratio – 10.24

Honeycomb Thickness/Cell Size/Cell Count – 1.75in / 0.25in / approx. 16380

Max Mean Air Velocity – 14.8m/s, 33.1 mph

Max Mean Output – 57.3 m³/min, 2020 ft³/min

Diffuser Angle – 8 degrees

Tunnel

The wind tunnel is 9ft 3in long and constructed of 24 gauge sheet metal. The test section is 32in long and is made from a single sheet bent into a square tube with an inner diameter of 10in. All other sections were constructed from four separate panels, and these panels were then assembled into their respective sections using 1/8 in pop rivets. One inch tabs on the top and bottom edges of the side panels were bent outward to 90 degrees, allowing the top and bottom sections to be attached without the rivets protruding into the tunnel. Due to the fact that the test section is a single piece with one inch wide overlaps a both edges of one corner, riveting directly into the tunnel was unavoidable in this section and also around the joints between the individual sections. However, to ensure minimal effect on airflow in the tunnel, these seams were riveted from the inside so that the protruding end of the rivet is positioned on the outside of the tunnel. Most of the joints between panels were sealed with industrial rated mastic duct sealant before being affixed to one



Riveting the settling chamber to the contraction section.

another, but additional beads were run along all joints and seams after final assembly and before strips of aluminum HVAC duct tape were applied. The tape served to cover the excess duct sealant along the seams where the sealant's uneven surface would otherwise increase skin friction along the surface and create abnormal drag in the radial extremities of the tunnel cross section. Tape was also used around the section joints in an effort to smooth the transitions from one section to another.

Due to equipment and methods of construction, and also to my personal lack of experience in working with sheet metal, many of the seams did not meet as closely as I had originally anticipated. Though the electric sheet metal shear kindly loaned to me by the University's Facilities Maintenance personnel were much faster and easier to use than a pair of hand snips would have been, the pieces were still cut without the aid of a guide or stop, and the electric shear had a tendency to slightly warp the edges as it cut, though this may have been largely due to the incompetence of the operator. The breaker used to bend the pieces of metal was built to construct 10 foot lengths of ductwork and so was much larger than needed for most of my bends. The breaker did have a stop that could be used to make fairly consistent angles for a given thickness of sheet metal, but because of its design it would have been ineffective for the small angle bend required for many of my panels, so I choose to forgo it's use. Due to these factors, many of the bend had to be corrected when to the panels were fitted



Using the sheet metal breaker to construct panels for the exit diffuser.

together and this led to slight but noticeable warping in some panels and created amplified problems when attempting to attach close-fitting joints, despite the fact that tolerances were normally on the order of 1/8 inch.

Upon inspection of the dimensions listed above, one might notice that both the contraction ratio and the diffuser angle are slightly larger than the optimal values, and this is due to the fact that the tunnel was shortened by about 1/4 of its originally planned size. This may have had a somewhat detrimental effect on the flow uniformities, but limited funds and laboratory space raised some concern about the practicality of a tunnel over twelve feet long.

Base

The base for the wind tunnels was built off of an old six foot lab table. The drawers were removed and two ten foot lengths of two by six framing lumber were bolted to the sides of the table just under the lip of the table top. The carriage bolts used to attach the two-by-sixes were also run through vertical pieces of two-by-four. Three foot lengths of quarter inch threaded rod were bolted to the vertical two-by-fours so that they supported both the top and bottom of the tunnel. Care was taken to drill holes through the two-by-fours so that there would be a slight bend in the rod and the provided tension would keep the tunnel secure and eliminate noise due to rattling, though some pieces of rod still required some bending to acquire the proper fit.



Wind tunnel base



Supports for the settling chamber

On the intake end of the table, three pieces of two-by-four were screwed into the horizontal supports to add strength and provide a base for the settling chamber, though this was somewhat unnecessary. A length of two-by-six was mounted to the end of the horizontal supports in the same manner and the fan was attached to this piece with a pair of heavy utility hinges. These hinges were screwed to the wooden base of the fan with the tip of the triangular hinge plate slid under the metal flange of the fan. This conveniently allowed both hinge and flange to be attached with a common screw, which was helpful due to the limited amount of clearance between the fan and the base, but required the hinges to be ground down to size. The reasoning behind hinging the bottom edge of the fan to the base was that it would allow easy access to the settling chamber should the honeycomb or screen need to be cleaned or replaced.

Fan

The fan selected for this tunnel is a 30 in whole house attic fan in a square wooden frame with a flange of heavy gauge sheet metal on the exhaust side. The frame houses a direct drive motor assembly attached to fan hub and secured with a set screw. The fan itself has three cambered blades, also made from sheet metal, and the whole unit is rated for an output of 5700 cubic feet per minute (cfm). A control box with a pull chain controlled cycled the fan motor between the off position, and a low and high speed setting. This limited the range of possible experimental velocities, so the power cable was connected to a variable output AC power supply with a maximum output of about 140 volts. This VariAC power supply allowed a much wider operating range, though performance suffered somewhat at extreme low or high velocities. A quick, back-of-the-envelope calculation predicted top centerline velocities in the neighborhood of about 40 m/s, or close to 90 mph. Of course, this calculation was incredibly optimistic as the power losses due to honeycomb, screens, and contraction were completely neglected, and maximum experimental velocities were only about 15 m/s, or about 33.5 mph.



View of the fan mounted on the wind tunnel. Heavy gauge wire mesh is stapled to the frame to prevent debris from getting sucked in.

Settling Chamber

The honeycomb used is a piece of 3000 series expanded nonperforated aluminum honeycomb core purchased from HoneyCommCore LLC. in Cattaraugus, NY. The core is 1.75 inches thick and has hexagonal cells $\frac{1}{4}$ inches in diameter. The core did not arrive in a frame, and because of the brittleness of the edges I thought it best to construct one. The frame was made from four pieces of sheet metal bent along the lengthwise edges to hold the core and also at the ends to allow the pieces to be secure to one another with rivets. Fitting the core into the frame proved to be rather difficult, but once fitted the honeycomb slid snugly into the settling chamber and was attached to the walls with a pair of

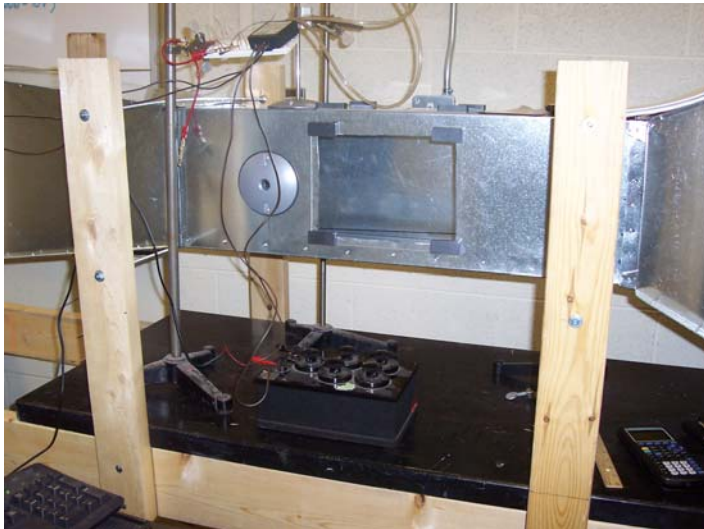


Settling chamber with both screens installed

screws on each side. Downstream of the honeycomb, I place a pair of aluminum screens to further even the flow. These screens were cut to size and then tacked to wooden frames made from 1.25 inch wide lengths of lumber. These lengths were cut from a piece of two-by-six lumber and then assembled using lap joint construction. The corners were secured with carpenter's glue and metal angle brackets anchored with drywall screws. The screens were stretched taught across the frame to minimize bowing and attached to the frames with a staple gun. The edges were planed and sanded to that the frame would fit in to the settling chamber, and they were secured to the walls in the same manner as the honeycomb.

Test Section

In the test section I cut two seven by nine inch rectangular holes for viewing windows, one in the top and one in the wall of the near side. These windows were covered by eight by ten pieces of Plexiglas-like impact resin. The plastic windows were secured to the tunnel with ceramic magnets placed at the corners. This is not the most secure or ascetically pleasing method of securing a viewing window, but it eliminated any unnecessary protrusions into the test sections, and pressure differences on either side of the tunnel wall are small enough that there is no real danger of the windows falling off or admitting appreciably disruptive jets of air into the working section. About four inches downstream of the viewing windows, I drilled to $\frac{3}{4}$ inch holes to allow the pitot tube to be inserted. Port covers with foam gaskets were riveted to the outside walls centered on the pitot tube holes. The holes are centered so that velocity measurements can be taken over vertical and horizontal cross sections or directly over test samples in the working section.



Test section of the tunnel. Viewing windows are secured with ceramic magnets and the pitot tube port covers are riveted directly to the tunnel. The variable resistor is on the table next the ring stand, which is holding the pressure transmitter.

The pitot tube is attached via aquatic tubing to a differential pressure transmitter. Data output from this transmitter is in the form of a small current. Lacking a reliable ammeter probe for the Vernier LabPro I was using to take data, I instead used a voltmeter probe to measure voltage drop across a resistor. The variable resistor used is a bit dated (the inspection sticker lists the calibration date 10-30-1968) but the knobs used to adjust the resistance were more precise than the other types of resistors available, which utilized a slide to vary resistance. The resistor was set to one kilo ohm, but the formula used to convert the voltage reading to a current usually require resistance values between 895 and 925 to obtain the correct

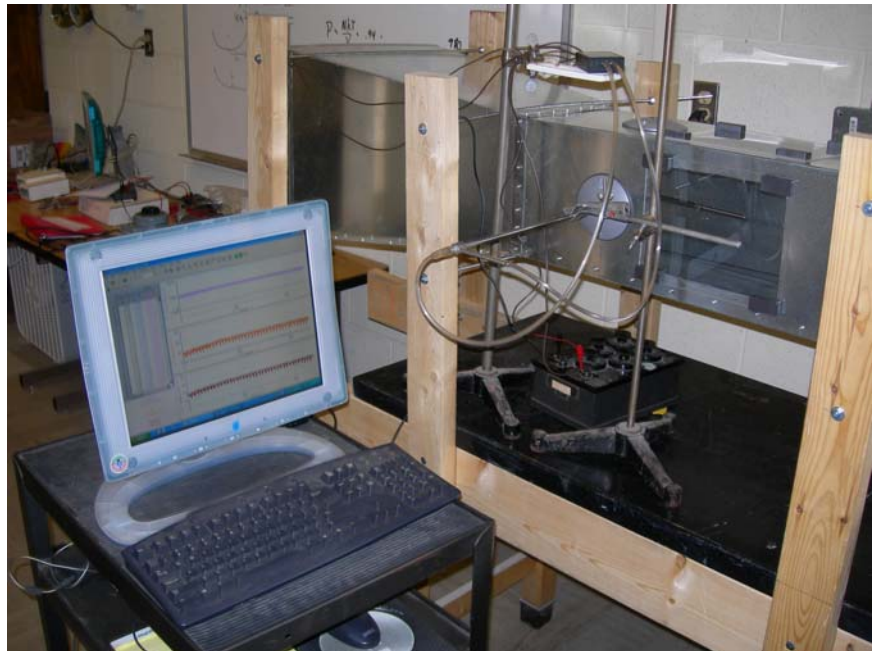
calibration. The current reading is then converted to a pressure value using the conversion provided by the manufacturer: 4mA is equal to 0 inches of water column, and the maximum output of 20 mA is equal to 3 inches of water column (1 inch of water column is equal to 249 N/m²). All other values can be obtained from extrapolation of this linear relation.

Because the pitot tube measure the difference in absolute pressures inside and outside the tunnel, the value obtained for the pressure reading does not include atmospheric or, in this case, static pressure. Thus, the pressure reading is the value of the dynamic pressure due to the fluids movement which is related to fluid velocity according to the formula below.

$$P = \frac{1}{2} \rho v^2$$

From this relation, air velocity in the tunnel can be calculated and, in turn, so too can the Reynolds numbers. Using known constants and the expression for the Reynolds number quoted earlier, the Reynolds value for my tunnel when empty is given by $R = 15580 \cdot \text{velocity}$. When I first calculated this number, I was alarmed by the size of this value relative to the Reynolds numbers I had been used to seeing associated with Oscar Reynold's experiments, all of which are on the order of 10^3 . After recalculating to make sure I had not made an error and pondering this seemingly inexplicable result for a short while I realized that

Oscar Reynolds conducted his experiments using water as a test fluid, and the difference in density and viscosity accounted for the larger Reynolds values. A quick web search also revealed that for wind tunnels, Reynolds numbers on the order of 10^5 (and even 10^6 in larger, high-velocity tunnels) are expected.

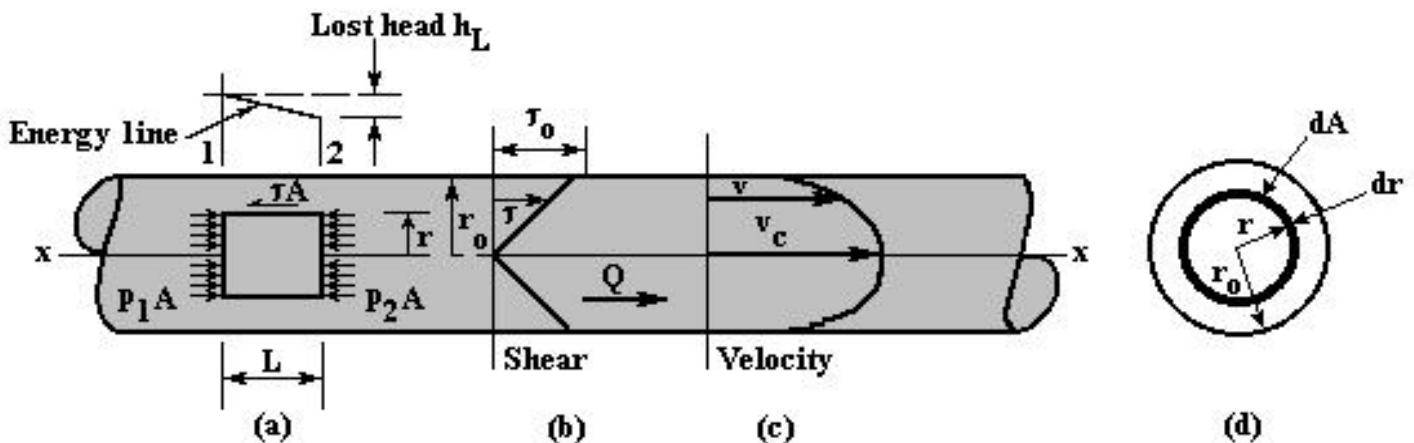


Taking data for the horizontal velocity profile.

Velocity Profile

The first data taken in the wind tunnel upon its completion was a vertical velocity profile, followed by a similar horizontal profile. For these profiles, data was taken at intervals recommended by the manufacturer, which were really intended for a circular tunnel and were not quite sufficient for my tunnel. The curves obtained in these profiles were mostly flat with slight downward curves at the ends. In both cases, the downward behavior was more pronounced next to the wall furthest from the viewing window and port, which I am currently at a loss to explain. These profiles also indicated that boundary layer behaviors was restricted to a distance of about 1.25 inches from the wall, and additional data points in this region were needed in order to see the proper parabolic behavior in velocities near the walls. New data was taken at 1/8 inch intervals in the inch closest to the walls and these showed a distinctly parabolic behavior, but did not match the predicted curves as closely as I had hoped. This may be due in part to the fact that the calculation for the parabolic velocity profile assumes a pipe with a circular cross section, and also because the size of the pitot tube does not allow measurements closer than about 1/8 inch from the wall.

Derivation of Parabolic Velocity Profile



I will now present the derivation of the velocity equation for Newtonian fluids flowing in a smooth pipe of circular cross-section. Writing the expression for shearing stresses on Newtonian fluids in the usual way and then assuming radial symmetry gives the following:

$$\tau = \mu \frac{dv}{dy} = -\mu \frac{dv}{dr}$$

Where $r = r_0 - y$. This equation can also be expressed using the specific weight of the fluid (γ) and the lost head (h_L).

$$\tau = \frac{\gamma h_L r}{2 L}$$

Applying boundary conditions, at $r = 0$, $\tau = 0$, while at $r = r_o$,

$$\tau = \frac{\gamma h_L r_o}{2 L} = \tau_o$$

Expressing the shearing stress equation as

$$\frac{dv}{dr} = -\frac{\tau_o r}{\mu r_o}$$

Integrating, and then imposing the no slip condition, which sets the velocity equal to zero at the walls of the pipe, yields

$$v = \frac{\tau_o}{2 \mu r_o} (r_o^2 - r^2)$$

But, we know that v must equal the centerline velocity when $r = 0$, so the previous equation can be written in terms of the centerline velocity.

$$v = v_C \left(1 - \frac{r^2}{r_o^2} \right)$$

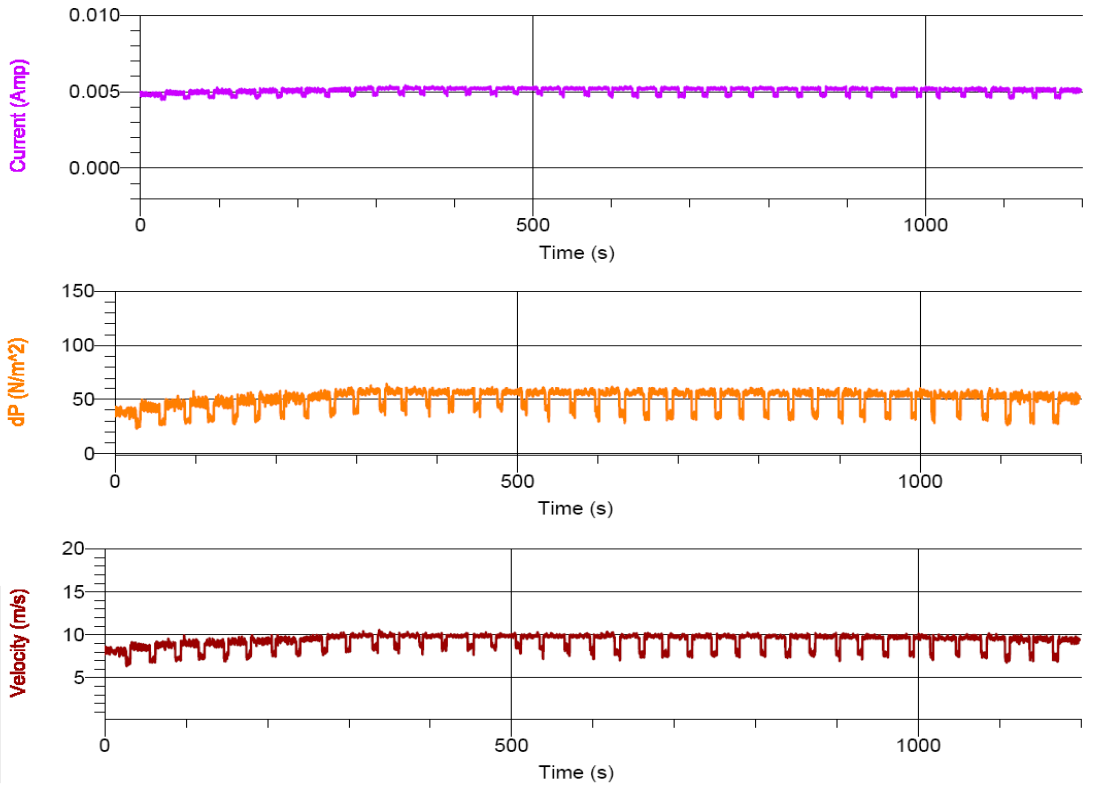
Velocity Profile Data

In order to take data for the velocity profiles the fan was kept at a constant setting and measurement were taken at incremental distances from the wall. The stem of the pitot tube was marked off in one inch increments, but because of the much smaller intervals needed to see the profile in any detail, a small transparent plastic ruler was used to adjust the tube. Because the pitot tube is supported by a metal clamp attached to a ring stand, it was practically impossible to adjust the pitot tube without twisting it and causing irregularities in the velocity readings. Also, the software program I used to record data did not allow data collection to be paused while the tube was being adjusted so in order to mark the locations where the tube was moved, I intentionally twisted the tube while shifting it. This resulted in a series of drops in the velocity readings occurring roughly every 60 seconds, as can be seen in the screen shot below.

Horizontal Velocity Profile Data

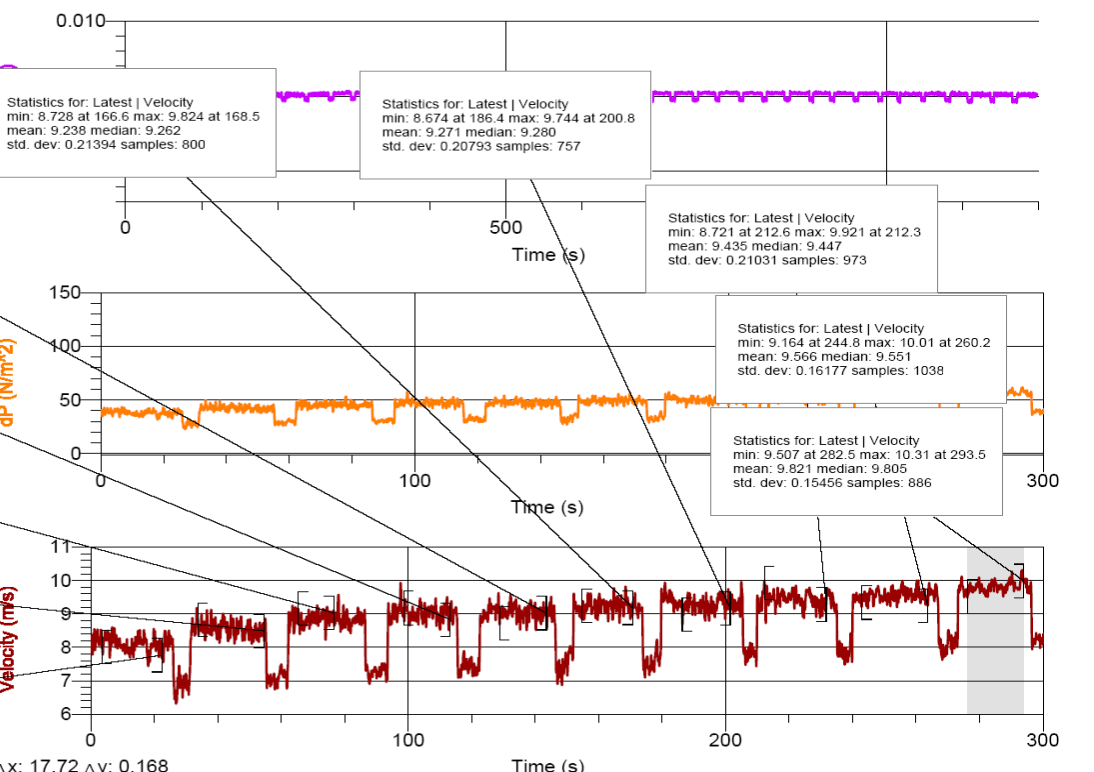
	Time (s)	Potential (V)	Current (Amp)	Latest dP (N/m ²)
1	0.02	4.046	0.00475	
2	0.04	4.261	0.00477	
3	0.06	4.520	0.00479	
4	0.08	4.691	0.00480	
5	0.10	4.276	0.00484	
6	0.12	4.364	0.00487	
7	0.14	4.139	0.00483	
8	0.16	4.598	0.00480	
9	0.18	4.574	0.00481	
10	0.20	4.242	0.00483	
11	0.22	4.232	0.00486	
12	0.24	4.379	0.00488	
13	0.26	4.657	0.00485	
14	0.28	4.476	0.00487	
15	0.30	4.603	0.00489	
16	0.32	4.105	0.00490	
17	0.34	4.393	0.00488	
18	0.36	4.549	0.00486	
19	0.38	4.647	0.00482	
20	0.40	4.383	0.00485	
21	0.42	4.134	0.00485	
22	0.44	4.237	0.00479	

Current
 0.00396 Amp
 dP
 -1.701 N/m²
 Velocity
 1.28 m/s



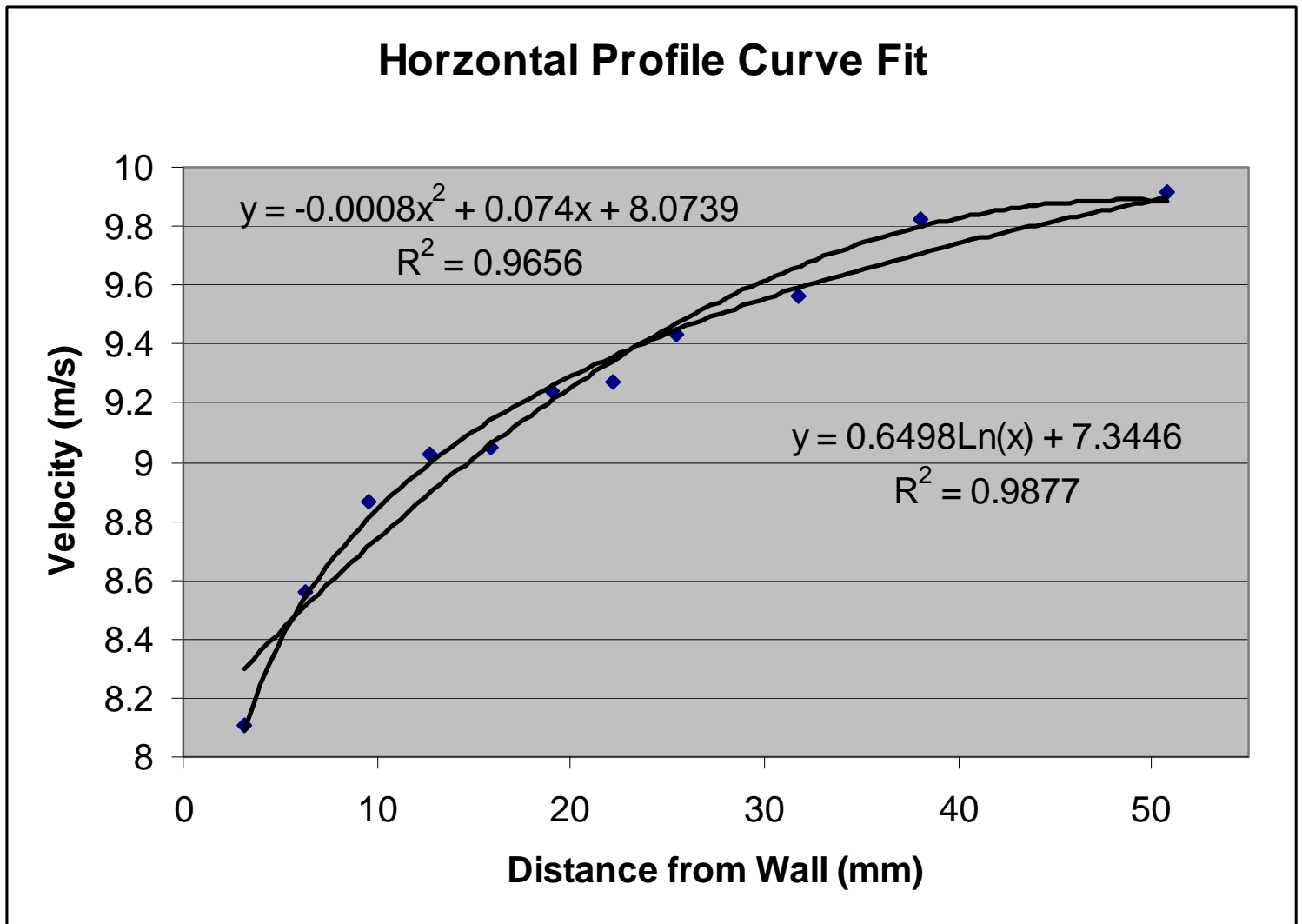
In order to analyze this data, I focused on a two-inch wide region adjacent to the far wall of the tunnel. The picture below shows data for the time averaged velocities in each incremental location.

	Time (s)	Potential (V)	Current (Amp)	Latest dP (N/m ²)
13812	276.24	4.799	0.00511	
13813	276.26	4.515	0.00516	
13814	276.28	4.545	0.00517	
13815	276.30	4.730	0.00516	
13816	276.32	4.930	0.00514	
13817				
13818				
13819				
13820				
13821				
13822	276.54	4.769	0.00513	
13823	276.56	4.647	0.00514	
13824				
13825				
13826				
13827				
13828				
13829				
13830				
13831				
13832	276.64	4.647	0.00514	
13833				
13834				
13835				
13836				
13837				
13838				
13839				
13840				
13841				
13842				
13843				
13844				
13845				
13846				
13847				
13848				
13849				
13850				
13851				
13852				
13853				
13854				
13855				
13856				
13857				
13858				
13859				
13860				
13861				
13862				
13863				
13864				
13865				
13866				
13867				
13868				
13869				
13870				
13871				
13872				
13873				
13874				
13875				
13876				
13877				
13878				
13879				
13880				
13881				
13882				
13883				
13884				
13885				
13886				
13887				
13888				
13889				
13890				
13891				
13892				
13893				
13894				
13895				
13896				
13897				
13898				
13899				
13900				

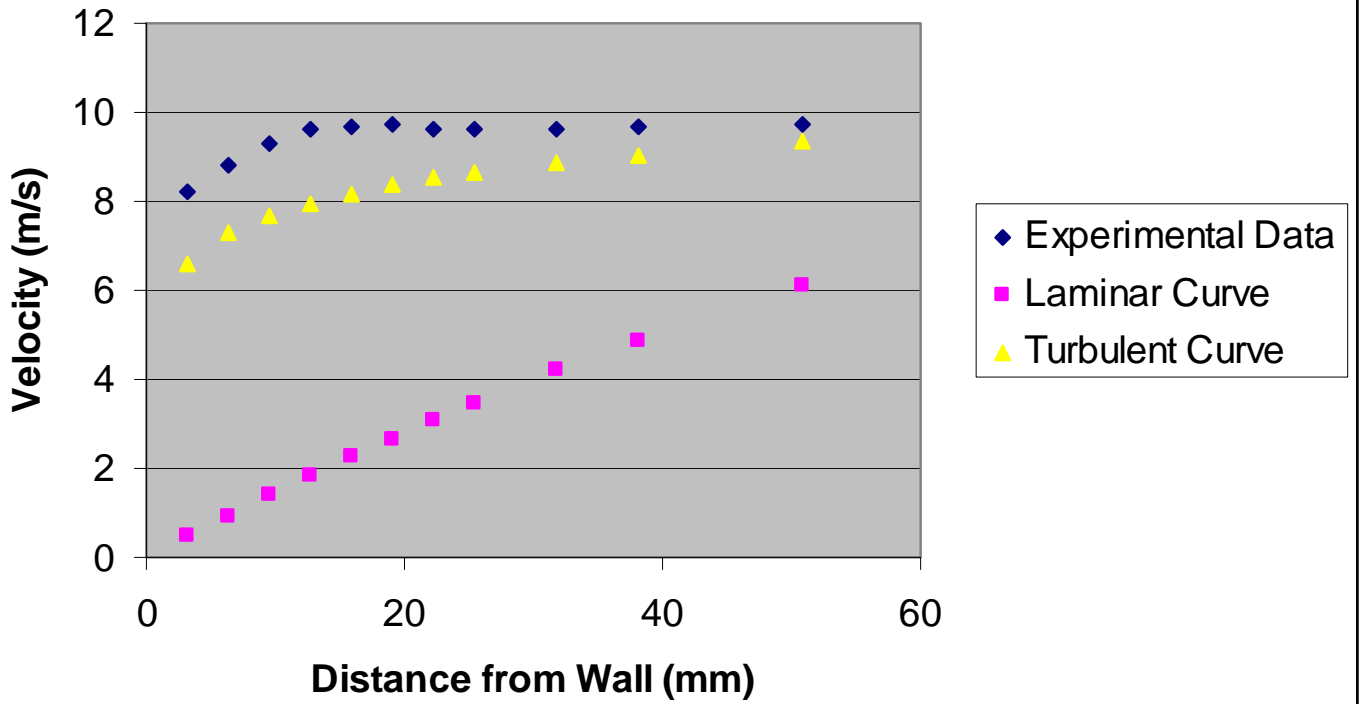


ΔX: 17.72 ΔY: 0.168

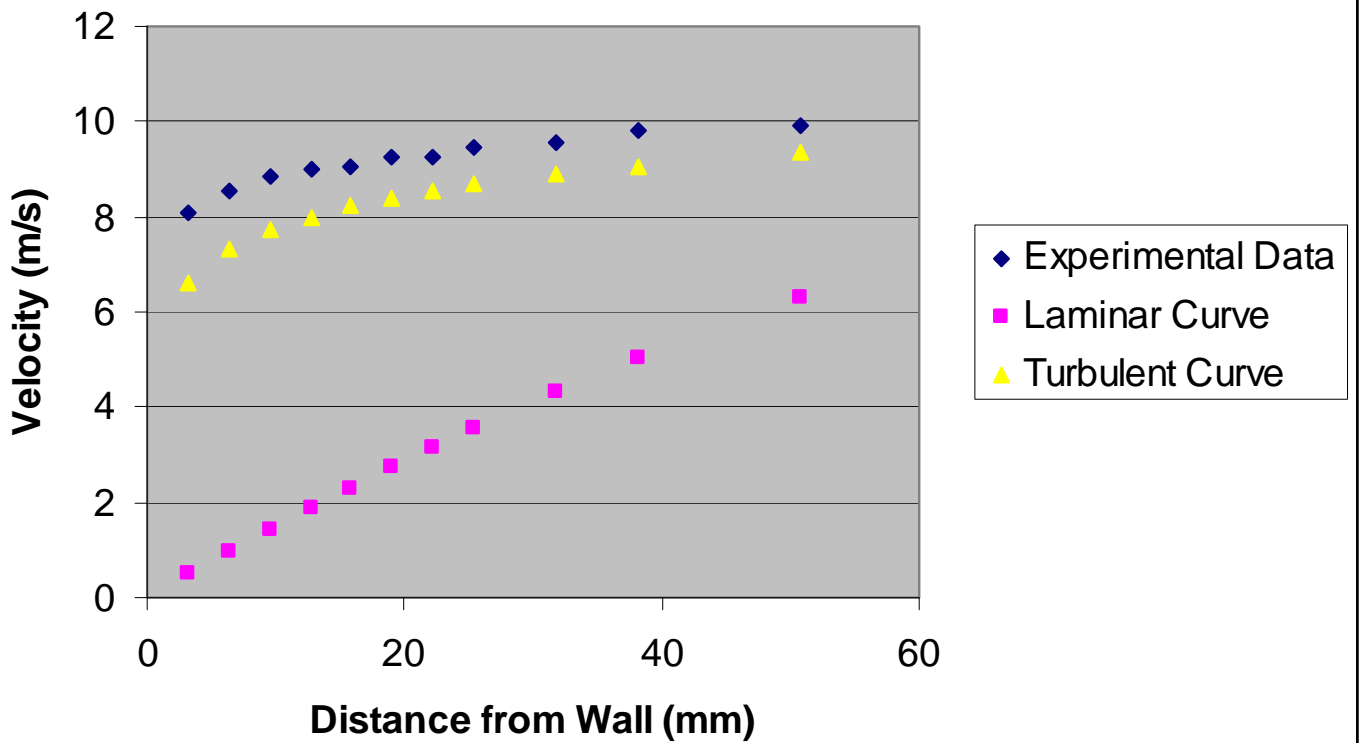
When plotting these mean velocities against distance from the wall of the tunnel, I initially expect to see a close match to the parabolic curve calculated using the equation for laminar flow in a smooth pipe derived above. I was little surprised to see a significant deviation between the two curves, due mostly to the fact that my experimental curve did not go to zero at the wall of the tunnel. This was a little concerning, but it is plausible that the experimental data would fall off to zero if measurements were taken closer to the wall. However, due to the thickness of the pitot tube, I could not take data any closer to the wall. I then found a derivation for an equation describing velocities for turbulent flow in a smooth pipe, and a quick plot of one of these curves looked much closer to my data than did the parabolic curve. I had anticipated laminar flow at the test velocities, which were all under 10 m/s, but it also seemed possible that the flow could be turbulent if the fan was inducing sufficient unsteadiness in the flow. A more precise plotting of the logarithmic curve was closer to my data, but there was still a noticeable amount of deviation. Fitting both a logarithmic and second-degree polynomial to my data curve revealed very little, as both curves displayed nearly identical R² values. Both curves for my horizontal profile are graphed below. For reasons that are still unclear, the horizontal data fit both curves much better than the vertical data, for which the fitted curves displayed R² values close to 0.75 instead of 0.97 for the horizontal curves.



Vertical Velocity Profile



Horizontal Velocity Profile



The derivation for the logarithmic velocity equation plotted in the graphs is rather arduous and involves a bit of hand-waving, so I will not present it here. Much of the equation, including the constant terms, is based upon experimental data taken in pipes of various roughness. There are actually two logarithmic equations (and probably many more), one for smooth and one for rough pipes, but according to tables found in my literature commercial metal can generally be considered smooth. Thus, I have used the following smooth pipe equation for all my graphs.

$$v = v_* \left(2.5 \ln \left(\frac{v_* y}{\nu} \right) + 5.5 \right) \quad v_* = \sqrt{\frac{\tau_o}{\rho}}$$

Porous Surface Flow

My initial motivation for constructing a wind tunnel was to examine fluid flow over a porous surface. The samples I used are actually a material recently developed by a local manufacturer and, due to its remarkable thermal properties, the manufacturer is trying to market the material to aircraft corporations for use as heat insulation inside jet engines. My plan for this project was to make some initial observations of flow properties at low speeds, and determine upper critical velocities, those at which the flow became turbulent. I also hoped to be able to determine the effects of pore size and density on both the air velocity at which turbulent flow developed and the severity of the turbulence produced. The former can be measured directly using a pitot tube to determine mean velocity within the tunnel, and this data can then be used to determine the Reynolds number. The latter was to be observed qualitatively through clear plastic viewing windows aided by the use of smoke/string, but due to limited time and resources this will probably have to be left to future investigation. As I have previously mentioned, Reynolds numbers must be determined experimentally using some other measure of turbulence to find acceptable critical numbers. Due to a mysterious temporal variation in velocities and the lack of visual aids, quantifying turbulent flow in my tunnel has proven to be exceedingly difficult. At best, only a rough estimate of turbulent flow velocities can be obtained. I had also hoped to determine some correlation between the upper critical velocity and the average size and density of the pores in the surface of my test material, but upon receiving the samples I realized that this would also be largely impractical. I had anticipated a fairly even surface with circular pores of some reasonably consistent size, but instead the samples had a highly irregular distribution of pores with no uniformity in size or shape. The only meaningful measure of the roughness of the surface is the density of the slab. I received eight samples, all about six inches square and 1.25 inches thick, with densities varying from 13.9 lbs/ft³ to 57.15 lbs/ft³ (223 kg/m³ to 915 kg/m³). The highest density slab is a great deal smoother than the rest, but the lower density slabs are about equally porous.

In order to prevent the samples from disturbing the flow, I constructed a sort of bracket with fairings on both ends in hopes of avoiding boundary layer separation and unnecessary turbulence. The bracket sits in the floor of the wind tunnel and has a flat surface about 16 inches long with gently sloped ramps about seven inches in length. It is nearly the same height as a sample laying flat on the bottom of the tunnel, and a six inch square opening cut in the center of the flat portion of the bracket allows the sample to drop through and rest on the floor. Thus flow passing over the sample is parallel to the surface with minimal disturbance in the flow.

For the first data run, a scrap piece of sheet metal was placed over the bracket hole in order to get a feel for the new velocities and check for flow instabilities. There was a slight increase in average velocity for a given voltage input which, given that the bracket essentially acts as a second contraction, was expected. However, I also noticed that after a minutes or two at constant velocity, a low frequency oscillation developed and reoccurred intermittently. This variation was significant, three or four meters per second at times, and had a periodicity of nearly a minute. This could not be caused by vibration within the tunnel, and all electrical and pneumatic connections were double checked. Power supplies for both the tunnel and the pressure transmitter were checked, as were the wall outlets, the LabPro module, the voltage probe and the variable resister. At a loss to explain the oscillations in the readings, my advisor contacted the manufacturer and spoke for some time with a company engineer who advised returning the unit for repair. The replacement unit did not arrive in time for me to take and data, so this portion of the project will have to be completed by a future student.

References

Auld, D.J., Srinivas, K. Aerodynamics for students.
<http://www.aeromech.usyd.edu.au/aero/>

Bradshaw P, Mehta RD. Design rules for small low speed wind tunnels. The Aeronautical Journal of the Royal Aeronautical Society November 1979

Celli, V. Sep 28, 1997. Viscosity effects at high Reynolds numbers.
<http://galileo.phys.virginia.edu/classes/311/notes/fluids2/node10.html>

Elert, G. 2006. The Physics Hypertextbook.
<http://hypertextbook.com/physics/matter/viscosity/>

Jackson, J.D. Reynolds the scientist.
<http://www.eng.man.ac.uk/historic/reynolds/oreynB.htm#OS421>

Johnston, D. Drag. U.S. Centennial of Flight Commission.
http://www.centennialofflight.gov/essay/Theories_of_Flight/drag/TH4.htm

Mehta RD. Turbulent boundary layer perturbed by a screen. American Institute of Aeronautics and Astronautics Journal Vol, 23, No. 9, September 1985

Navier-Stokes equations: 3 dimensional unsteady. NASA Glenn Research Center.
<http://www.grc.nasa.gov/WWW/K-12/airplane/nseqs.html>

Talay, T. A. Introduction to the Aerodynamics of Flight.
<http://history.nasa.gov/SP-367/cover367.htm>

Vennard J, Street R. 1982. Elementary Fluid Mechanics (6th ed.). New York (NY): John Wiley & Sons.

Weisstein, E.W. Boundary layer.
<http://scienceworld.wolfram.com/physics/BoundaryLayer.html>

Weisstein, E.W. Navier-Stokes equations.
<http://scienceworld.wolfram.com/physics/Navier-StokesEquations.html>

Weisstein, E.W. Reynolds number.
<http://scienceworld.wolfram.com/physics/ReynoldsNumber.html>

Picture Credits

1. http://www.centennialofflight.gov/essay/Theories_of_Flight/Real_Fluid_Flow/TH9G2.htm
2. <http://exploration.grc.nasa.gov/education/rocket/Images/boundlay.gif>
3. <http://navier.stanford.edu/bradshaw/tunnel/fig/Fig2.html>
4. http://www.etw.de/windtunnel/ac/etw_sceme750.jpg
5. http://www.adl.gatech.edu/classes/lowspdaero/lospd2/lospd2_files/image046.gif
6. http://www.engr.umd.edu/facilities/images/fa_gmwt-fanfront.jpg
7. <http://navier.stanford.edu/bradshaw/tunnel/photo/pages/photo06.html>
8. <http://www.core.org.cn/OcwWeb/Mechanical-Engineering/2-26Spring2004/CourseHome/>
9. <http://www.mhi.co.jp/kobe/mhikobe-e/products/etc/siken/low/kemuri/>